

# Retinal optic disc and blood vessels: the segmentation of overlapping tissues

**Abstract**—The overlapping of tissues is a common case in the analysis of medical images. In particular the retinal optic disc is overlapped by the blood vessel network, and this makes difficult the segmentation of these structures. In this paper we address the overlapping issue by exploring two opposing research lines. As most of the current method in the literature our system detects blood vessels as a first step. By detecting the convergence of vessels the optic disc is localized. In this stage two different approaches are explored, incorporation and discrimination of vessels as part of the formulation for the optic disc segmentation. In the case of vessels incorporation we make use of our previous work [8], where prior segmented vessels are used to incorporate an additional constraint into a graph formulation. On the second case vessels are discriminated by using a MRF reconstruction; as a result a well defined optic disc is generated and its segmentation is performed then. Our methods were tested on two public datasets, DIARETDB1 and DRIVE. The analysis of experimental results provides new knowledge to attend the segmentation of overlapping tissues.

**Index Terms**—Graph cuts, retinal images, optic disc, retinal blood vessels

## I. INTRODUCTION

The number of people with retinopathy symptoms has increased considerably in recent years. Early adequate treatment has demonstrated to be effective to avoid the loss of the vision. The analysis of retinal images represents a non invasive alternative for periodical eye screening. The morphology of retinal structures (optic disc and blood vessels) is an indicator of the actual condition of the eye. The segmentation of these structures is the first step in order to extract features that can be evaluated.

The main issue to attend is the fact that optic disc and blood vessels are overlapping tissues. This is a common case in the analysis of medical images. Most of the current methods in the literature have addressed this issue by discriminating the vessels from the process to segment the optic disc. Some other methods do not have any special processing to attend this issue.

In this paper we address the overlapping issue by exploring two opposing research lines. As most of the current method in the literature our system detects blood vessels as a first step. By detecting the convergence of vessels the optic disc is localized. In this point two different approaches are explored, incorporation and discrimination of vessels as part of the formulation for the optic disc segmentation. In the case of vessels incorporation we make use of our previous work [8], where prior segmented vessels are used to incorporate an additional constraint into a graph formulation. On the second case vessels are discriminated

by using a MRF reconstruction; as a result a well defined optic disc is generated and its segmentation is performed then.

Firstly we make a review of the relevant literature about the segmentation of the retinal optic disc and how the overlapping of vessels issue has been attended by other methods. Section III presents an overview of our research work and details the main procedure. Section IV and V are dedicated to present the opposing methods, discrimination and incorporation of vessels as part of the process to segment the optic disc. Finally section VI presents the experimental work and the results.

## II. BACKGROUND

In [1] a combination of morphological operations, Hough transform and an anchored active contour model is used to segment the optic disc. The blood vessels are removed by using a distance map; each pixel is assigned a value equal to its distance from the nearest boundary. This distance map is then thresholded and all pixels with a distance of six or less are removed. The method assumes a maximum vessel diameter of ten pixels, which produce a distance of five, but this is not always the case for all retinal images datasets. A deformable contour model is used to segment the optic disc in [5]. The model makes use of a direction-sensitive gradient which try to ignore vessel edges distraction. The watershed transform form markers is used to find the optic disc boundary in [11]. A first boundary is found by using initial makers, later by using an iterative process markers are updated and new boundary is defined. In order to minimize the vessel obstruction in the internal marker the method performs morphological erosion. In [3] the optic disc boundary is localized by using morphological and edges detection techniques followed by a Circular Hough Transform. The authors consider the blood vessels within the optic disc as a strong distracter and indicate that they should be erased. The method makes use of morphological processing to eliminate vessels.

In [12] blood vessels are used to estimate the location of the optic disc. The retinal vessels are segmented by using a 2-D Gaussian matched filter and a vessel direction map is created. The vessels are then thinned, and filtered using local intensity, to finally represent the optic disc centre candidates. The minimum difference between the matched filter result and the vessel direction around each candidate provides an estimation of the optic disc location. The method just localize the optic disc, but it does not perform its segmentation.

In [9] the histogram of the enhanced retinal image is modelled using a mixture model. From the histogram shape,

two heavy tails are distinguished and assumed as foreground area (vessels, optic disc and lesions). It is assumed that the high intensity tail includes the optic disc. From the high intensity tail optic disc is segmented. The segmentation is performed by using mathematical morphology to select candidate pixels; this selection is then pruned by restricting the selection to the pixels in the neighbourhood of the main vessels. The main vessels are detected by using a two dimensional vertical oriented filter. The method assumes that the primary four vessels normally emanate near vertically from the optic disc. This assumption limited the performance of this method to the type of retinal images where the optic disc has been captured under the exact conditions to clearly display the four main vessels crossing vertically the optic disc.

Morphological operations are a recursive element to eliminate vessels from the retinal image beforehand [11, 3]. But this type of processing operates not only on vessels, the modification is extended to the rest of the image and some important information can be corrupted. This issue has been pointed out in [3], which declares that as a consequence of this processing the optic disc is enlarged by a fixed length in all directions.

In our discrimination of vessels method we remove vessels from the ROI by using prior vessel segmentation to perform the reconstruction of the image. The reconstruction is performed only on the vessel pixels (unknown pixels) to avoid the modification of other structures. Our proposed methods were designed as unsupervised methods, and they can perform on images with different characteristics. In the next section the process to localize the optic disc is explained. Next, the problem of segmenting overlapping tissues is presented and the methods to explore the opposing research lines are detailed.

### III. OPTIC DISC LOCALIZATION

Inspired by the work presented in [11] we use the segmented vessel network to localize the optic disc. The binary image is pruned by using a morphologic open process in order to keep the main arcade. Afterwards the centroid of the arcade is located using the following formulation:

$$C_x = \sum_{i=1}^K \frac{x_i}{K} \quad C_y = \sum_{i=1}^K \frac{y_i}{K} \quad (1)$$

where  $x_i$  and  $y_i$  are the coordinates of the pixel in the binary image and  $K$  is the number of pixels set to "1", which is the pixels marked as blood vessels in the binary image.

Using the gray intensity of the retinal image, 1% of the brightest pixels are selected. The algorithm detects the brightest area with the most number of elements in the image to determine the position of the optic disc with respect to the centroid (left, right, up, down, etcetera). Considering that the main arcade is narrowing until the vessels converge, the algorithm adjusts the centroid point iteratively until it reaches

the centre of the arcade.

The centroid point is then adjusted by reducing the distance with the optic disc, and correcting its central position inside the arcade. The centre of the arcade is presumed to be the vessels convergence point and the centre of the optic disc. Figure 1 shows an example of the localization process of the optic disc centre. It is important to detect with accuracy a point inside of the optic disc, since this point will be used to automatically mark foreground seeds. A point just inside the border of the optic disc may result in some false foreground seeds.

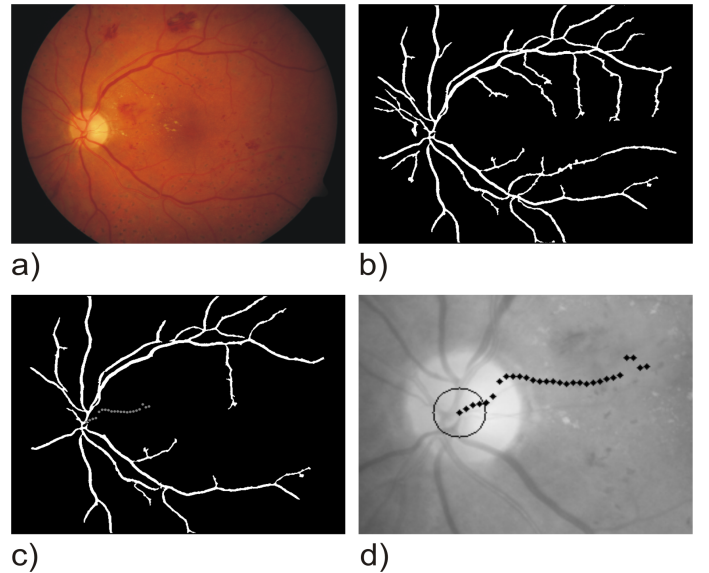


Fig. 1: Optic disc localization. a) retinal image, b) blood vessel segmentation, c) blood vessel segmentation after pruning and d) sequence of points from the centroid to the vessels convergence.

We constrain the image to a small area in order to minimize the processing time. The region of interest (ROI) is constrained to a square of 200 by 200 pixels concentric with the detected optic disc centre. We have selected an automatic initialization of seeds (foreground and background) for the graph. A neighbourhood of 20 pixels of radius around the centre of the optic disc is marked as foreground pixels, while a band of pixels around the perimeter of the image are considered as background seeds(see Figure 2).

### IV. SEGMENTATION OF OVERLAPPING TISSUES

The retinal blood vessels have a double role in the optic disc segmentation. On the one hand, blood vessels break the continuity of the optic disc creating an obstruction for its segmentation; and on the other hand blood vessels inside the optic disc are part of the object to be segmented. The overlapping of tissues is a common issue to address in the analysis of medical images.

Figure 3 shows some retinal images where the optic disc was segmented using the traditional formulation of the graph

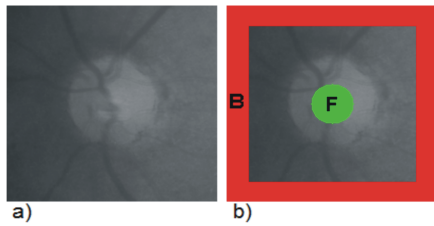


Fig. 2: a) constrained image, b) foreground **F** and background **B** seeds initialization in the constrained image.

cut technique. Note that blood vessels interrupt the continuity in the segmentation of the optic disc. The high contrast of vessels inside of the optic disc misguides the segmentation through the shortest path.

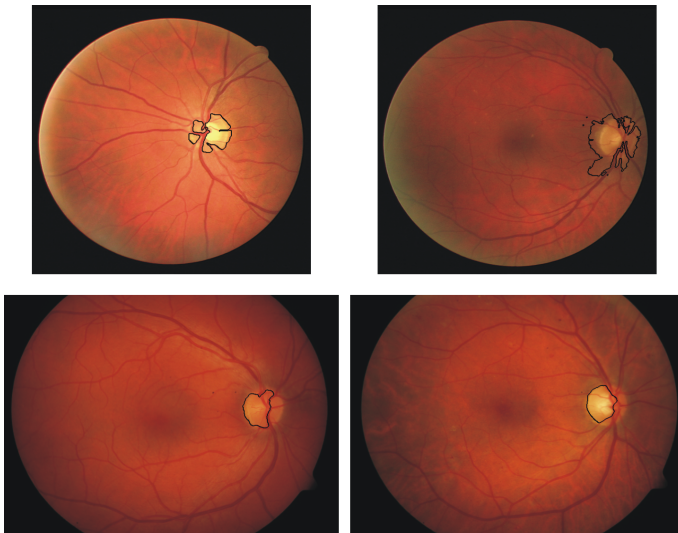


Fig. 3: Retinal optic disc segmented using traditional formulation of graph cut technique. Top: DRIVE dataset samples; bottom: DIARETDB1 dataset samples.

For the reason exposed above the segmentation of the optic disc process requires of special attention for the blood vessels. There are two main premises by using prior blood vessel segmentation, eliminate them prior to the segmentation process and incorporate them into the formulation technique. By exploring this opposing research lines the study is extended to cover both premises and the results could be used as guideline for other overlapping structures cases. Our proposed methods are based on these two premises and they are summarized next.

- **Discrimination of vessels (MRF reconstruction).** Prior blood vessels segmentation is used to perform a MRF reconstruction. Vessels pixels are considered as unknown, and the rest of the image is used to find the statistical best matching to substitute the missing pixels. As a result the optic disc appears as a well defined round bright object and is ready to segment. Traditional Graph

formulation is then used to segment the optic disc in the reconstructed image.

- **Incorporation of vessels (Graph Cut with compensation factor  $V_{ad}$ ).** While most of the methods for the optic disc segmentation have addressed this problem by trying to eliminate the vessels, we have incorporated them into the formulation. We introduced a compensation factor in the graph cut technique. The compensation factor is calculated by using prior vessel segmentation.

In both methods the convergence of the blood vessels is localized and assumed as the centre of the optic disc. Seeds are initialized automatically and used to create a general pixel intensity template for foreground and background. Foreground seeds are taken from the centre of the optic disc and Background seeds from a perimeter band.

## V. DISCRIMINATION OF VESSELS

In our first method the segmented vessels are discriminated from the retinal image. Figure 4 shows the methodology of our method. First vessels are segmented and used to localize the optic disc. Then the blood vessels are reconstructed by using MRF formulation. Vessel pixels are considered as unknown and the statistical best matching pixel is found to substitute the missing pixel. Later traditional graph cut formulation is used to segment the resultant well defined optic disc in the reconstructed image.

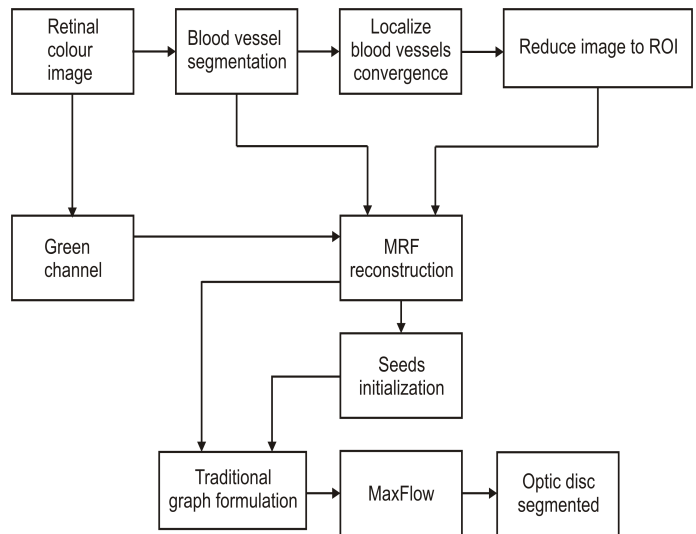


Fig. 4: Graph cut optic disc segmentation methodology using prior MRF reconstruction.

The MRF reconstruction is performed using previous blood vessel segmentation. Blood vessel pixels are considered as unknown and the surrounded pixels are used to fill these vacancies. We have selected Markov Random Field based reconstruction technique because of its robustness. The general idea is to find the best matching for the missing pixels. One of the disadvantages of this approach is the

intensive computation required. We address this problem by limiting the reconstruction to the region of interest. The method is summarized in Table I.

|   |
|---|
| Input: Colour retinal image $I_{in}$                        |
| 1. Segment the blood vessels from $I_{in}$ [7];             |
| 2. $I_c$ = Localize the optic disc and constrain the image; |
| 3. $I_r$ = Perform the MRF reconstruction of $I_c$ ;        |
| 4. Initialize $Fg_s$ and $Bg_s$ in $I_r$ ;                  |
| 5. $I_{out}$ = Construct graph for $I_r$ and resolve;       |
| Output: Optic disc segmented $I_{out}$                      |

TABLE I: Optic disc segmentation process using prior MRF reconstruction.

### A. MRF Reconstruction

In order to minimize the obstruction of blood vessels through the optic disc segmentation process we performed a reconstruction using prior vessels segmentation. As a result the reconstructed image provided a well defined optic disc. Later a traditional formulation of the graph cut technique is used to segment the optic disc.

Using prior blood vessel segmentation we perform the reconstruction in the ROI. We have selected a Markov Random Field based method to perform the reconstruction [2] for its robustness. In the beginning blood vessel pixels are considered as unknown. The general idea is to find a collection of patches statistically similar to the patch where a pixel  $p$  ( $p = 0$ ) is missed. Then we create a histogram of the pixels that are in the same position as  $p$  in the collection of patches and obtain the best approximate value to substitute the missing pixel.

A pixel neighbourhood  $w(p)$  is defined as a square window of size  $W$ , with centre on pixel  $p$ . The image that is going to be reconstructed is  $I$ . Some of the pixels in  $I$  are missing and the objective is to find the best approximate value for them. Let  $d(w_1, w_2)$  indicate a perceptual distance between two patches that indicate how likely they are. The exact matching patch would be the one that  $d(w', w(p)) = 0$ . If we define a set of these patches as  $\Omega(p) = \{\omega' \subset I : d(\omega', \omega(p)) = 0\}$  the probability density function of  $p$  can be estimated with a histogram of all centre pixel values in  $\Omega(p)$ .

But owing to the fact that we are considering a finite neighbourhood for  $p$  and the searching is limited to the image area, there might not be any exact matches for the patch. For this reason in our implementation we find a collection of patches whose match falls between the best match and a threshold. The closest match is calculated as  $\omega_{best} = \operatorname{argmin}_{\omega} d(\omega(p), \omega) \subset I$ . And all the patches  $\omega$  with  $d(\omega(p), \omega) < (1 + \epsilon)d(\omega(p), \omega_{best})$  are included in the collection  $\omega'$ . In our implementation  $d(w', w(p))$  is defined as the sum of the absolute differences of the intensities between patches, so identical patches will result in  $d(w', w(p)) = 0$ . We have set  $\epsilon = 0.1$  and  $W = 5$ . Using the collection of patches we create a histogram and select the one with highest

mode.

The reconstruction starts with the unknown pixels with most number to know pixels. In this way the patch represents with more accuracy the neighbourhood intensity distribution and the image is actualized after each unknown pixel is filled. Table II shows the pseudo function for the MRF image reconstruction.

The success of the reconstruction process depends in part of the segmentation of the blood vessels. Simply vessel sections that are not detected cannot be reconstructed. Figure 5 shows some examples of reconstructed images. It is possible appreciate the segmented vessels and their reconstruction on the retinal images. The optic disc appears as a well defined object in the reconstructed images and it ready to segment.

|   |
|---|
| Inputs: Retinal gray scale image $I_g$<br>and binary blood vessel image $I_{bv}$ .                                |
| 1. If $I_{bv}(p) = vessel$ then $I_g(p) = 0$ ;  |
| 2. Create a list of unknown pixels $p$ in $I_g$ ,<br>$I_g(p) = 0$ and their neighborhood $w(p)$ ;                 |
| 3. Sort out the list according with the number of<br>unknown pixels included as part of the neighborhood $w(p)$ ; |
| 4. for $i = 0$ to $i = W - 1$ ;   |
| for each element in the list;   |
| $patch = w(p)$ if unknown neighbors number is equal to $i$ ;  |
| find $\omega_{best} = \operatorname{argmin}_{\omega} d(\omega(p), \omega) \subset I$ ;                            |
| collection of patches $d(\omega(p), \omega) < (1 + \epsilon)d(\omega(p), \omega_{best})$ ;                        |
| create a histogram of collection of patches;  |
| Substitute $p$ in $I_g$ by the intensity with highest mode;   |
| $i++$   |
| end for   |
| end for   |

TABLE II: Pseudo function for the MRF image reconstruction in the constrained retinal image.

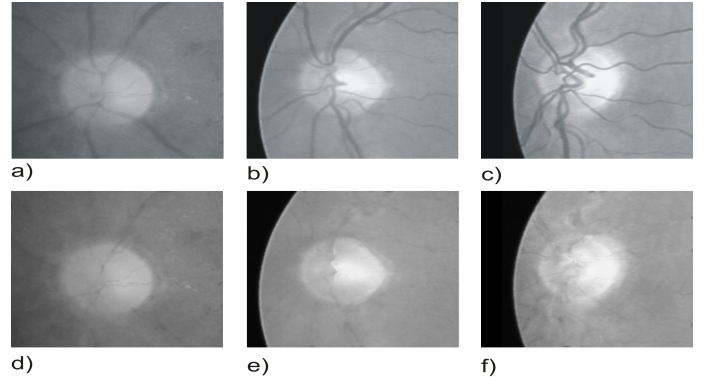


Fig. 5: MRF reconstruction applied to retinal images. First row: original gray scale images, second row: reconstructed images using the MRF based method

## VI. INCORPORATION OF VESSELS (GRAPH CUT WITH COMPENSATION FACTOR $V_{ad}$ )

The second method proposes the incorporation of vessels into the graph formulation by using a compensation factor  $V_{ad}$ . Figure 6 shows the algorithm for the method. Retinal green channel, blood vessels and the ROI are needed for the

graph construction. The graph formulation is limited to the ROI.

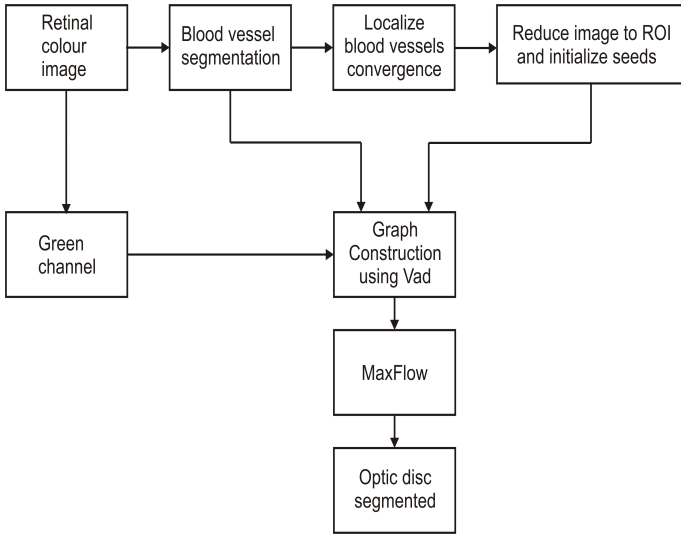


Fig. 6: Optic disc segmentation methodology using Graph cut technique with compensation factor  $Vad$ .

We have selected the traditional edge weight assignment method as base for our formulation [8]. Prior blood vessel information is incorporated to the graph formulation using a compensation factor  $Vad$ .

The energy function consists of regional and boundary terms. Regional term is calculated from the likelihood of a pixel  $p$  belonging to the foreground and background generating the t-link weights. The boundary term is based on the own pixel properties (i.e. intensity), which is used to assign weights to the n-links. For our particular purpose we have designed a compensation factor for the foreground t-link. The original image is constrained to a ROI concentrating the analysis in a smaller area and minimizing the processing time. The ROI is centred on the optic disc. The constrained image is preprocessed by applying a histogram equalization in order to enhance its contrast. Details about Graph Cut with compensation factor  $Vad$  method can be found in [8]

## VII. EXPERIMENTS AND RESULTS

Both methods were tested on two public datasets, DIARETDB1 [4] and DRIVE[10]. Our algorithm detected the optic disc centre successful in 96.7% on the DIARETDB1 dataset and in 97.5% of the images on DRIVE. The localization of the optic disc is used to initialize foreground and background seeds.

We created hand labelled sets for DIARETDB1 and DRIVE in order to have a ground truth to compare our results. The performance of the methods was evaluated by the overlapping ratio ( $Oratio$ ) and the mean absolute distance( $MAD$ ). The overlapping ratio is defined as:

$$Oratio = \frac{G \cap S}{G \cup S}$$

where  $G$  represents the manually segmented area and  $S$  is the area as result of the algorithm segmentation.  $MAD$  is defined as:

$$[MAD(G_c, S_c) = \frac{1}{2} \{ \frac{1}{n} \sum_{i=1}^n d(g_{ci}, S) + \frac{1}{m} \sum_{i=1}^m d(s_{ci}, G) \}]$$

where  $G_c$  and  $S_c$  are the contour of the segmented area in the ground truth and the resulting images, and  $d(a_i, B)$  is the minimum distance from the position of the pixel  $a_i$  on the contour  $A$  to the contour  $B$ . A good segmentation implies a high overlapping ratio and a low  $MAD$  value.

We calculated the sensitivity of the methods when they are applied to DIARETDB1 and DRIVE, which is defined as:

$$Sensitivity = \frac{Tp}{Tp + Fn}$$

where  $Tp$  and  $Fn$  are the number of true positives and the number of false negatives respectively. Sensitivity is an indicator of the foreground pixels detected by the segmentation method.

Our results are compared to those provided in [11]. This method was tested on the same datasets (DIARETDB1 and DRIVE) and results were measured under the same parameters. Also we have included the results of our experiments using the traditional graph cut technique without compensation and the ones using the topology cut technique [13].

Unfortunately most of the methods do not use a unique ground truth to measure the results of the optic disc segmentation, so this makes the comparison of the results difficult.

Figures 7 and 8 present the segmentation results using different methods on DIARETDB1 and DRIVE datasets. The manually labelled images have been included to have a visual reference. It can be seen that our method performs better over the blood vessel interference. Particularly the traditional graph cut technique tends to segment the optic disc along the blood vessels edges. The topology cut technique succeeds in the brightest area of the optic disc where the blood vessels are more likely to look like part of the foreground. The topology cut technique was applied to the color image directly without any preprocessing. The topology cut is not an automatic technique, and it requires a manual marking of foreground seeds.

Table III and Table IV show the comparison with different methods in terms of  $Oratio$ ,  $MAD$  and  $Sensitivity$ . Our method achieved the highest overlapping ratio with the minimum  $MAD$  value. It can be seen that an increase in the overlapping ratio does not mean a decrease on  $MAD$

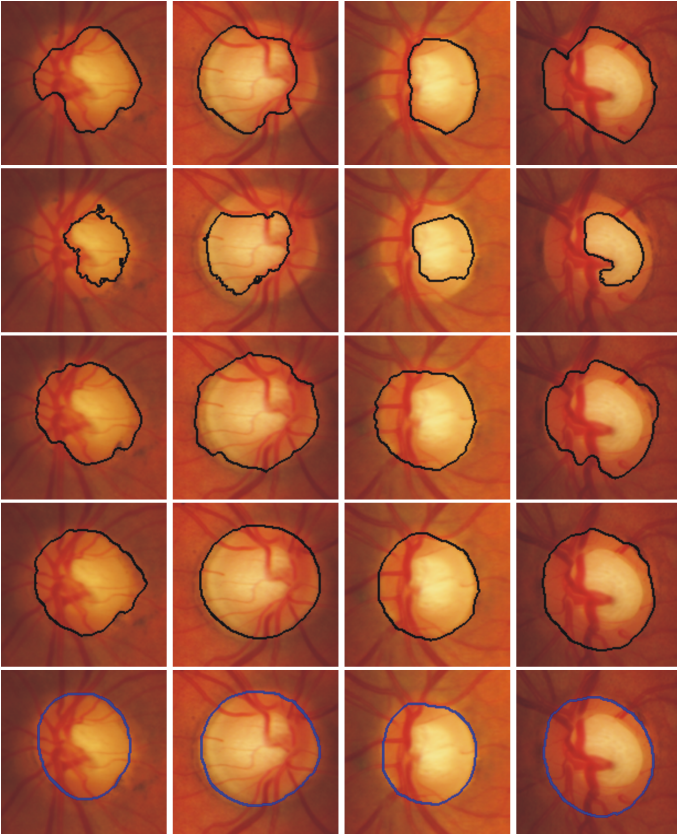


Fig. 7: Optic disc segmentation using different methods for DIARETDB1 dataset. First row: Topology cuts, second row: Graph cut, third row: Graph cut with compensation factor  $V_{ad}$  for blood vessels, fourth row: MRF + graph cut and fifth row: hand labelled

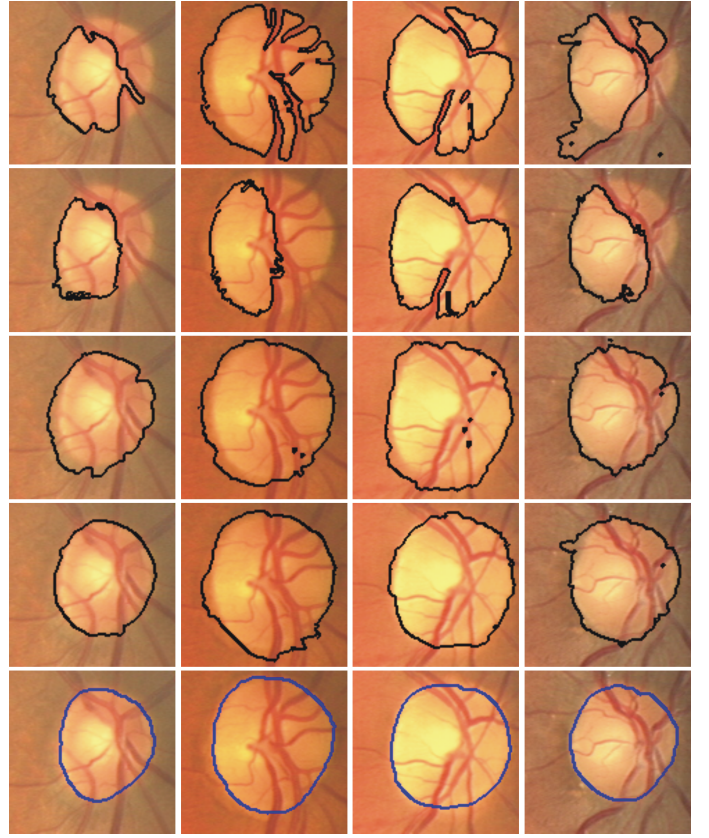


Fig. 8: Optic disc segmentation using different methods for DRIVE dataset. First row: Topology cuts, second row: Graph cut, third row: Graph cut with compensation factor  $V_{ad}$  for blood vessels, fourth row: MRF + graph cut and fifth row: hand labelled

value necessarily.  $MAD$  value does not represent the best way to measure the segmentation results, but it provides a good reference of the contour matching with the ground truth contour reference.

TABLE III: Performance comparison on the DIARETDB1 dataset.

| Method                    | Average ORatio | Average MAD | Average Sensitivity |
|---------------------------|----------------|-------------|---------------------|
| Topology Cut              | 38.43%         | 17.49       | 55.30%              |
| Adaptive morphologic [11] | 43.65%         | 8.31        | —                   |
| Graph Cut                 | 54.03%         | 10.74       | 76.35%              |
| Graph Cut with $V_{ad}$   | 75.74%         | 6.38        | 86.55%              |
| MRF + Graph Cut           | 78.3%          |             | %                   |

TABLE IV: Performance comparison on the DRIVE dataset.

| Method                    | Average ORatio | Average MAD | Average Sensitivity |
|---------------------------|----------------|-------------|---------------------|
| Topology Cut              | 55.91%         | 10.24       | 65.12%              |
| Adaptive morphologic [11] | 41.47%         | 5.74        | —                   |
| Graph Cut                 | 55.32%         | 9.97        | 73.98%              |
| Graph Cut with $V_{ad}$   | 70.70%         | 6.68        | 84.44%              |
| MRF + Graph Cut           | 82.2%          |             | %                   |

Figures 9, 10, 11 and 12 show the distribution of the overlapping ratio on DIARETDB1 and DRIVE using the four different segmentation methods. We have included lines as a reference at  $Oratio = 50\%$  and  $Oratio = 70\%$ . By using this reference lines it is possible appreciate the amount of

image segmented over an  $Oratio = 50\%$  and  $Oratio = 70\%$

There are few specific cases where the segmentation of the optic disc resulted in null by using our methods. These cases are shared by the other methods as well. The characteristic of these images is the poor contrast, as a consequence all the pixels are linked with strong weight and is not possible to find a cut to segment it. This is an indication of the challenge of analyzing those specific images.

In these specific cases it is possible to address the problem by adjusting the parameters in the energy function and the edge weight assignment to attend the specific needs of these images. This change will move our methods from automatic to interactive mode, where the user can adjust parameters for each image analysis.

Following the suggestion in [6], which takes a minimum overlapping ratio of 50% as a successful segmentation. Table V presents the success of the methods based on this assumption ( $Oratio > 50\%$ ).

Figures 13 and 14 show the cumulative histograms comparison, for normalized overlapping ratio on DIARETDB1 and DRIVE datasets using different methods. The cumulative histogram shows the frequency of the  $Oratio$  value when

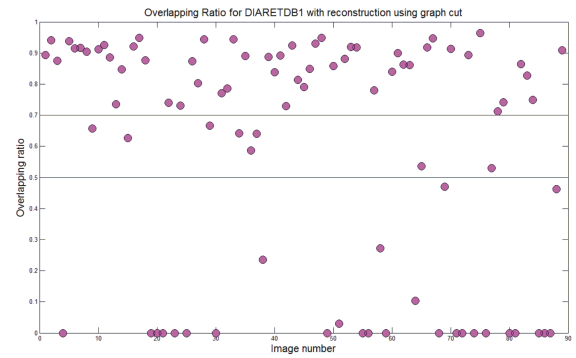
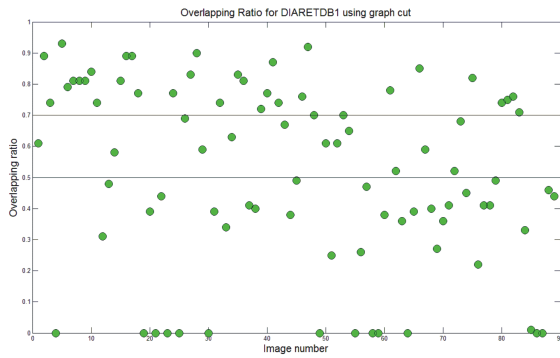
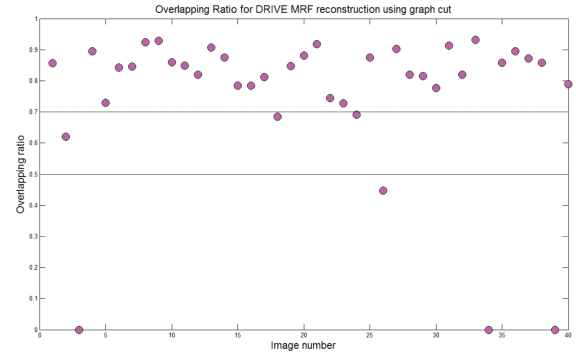
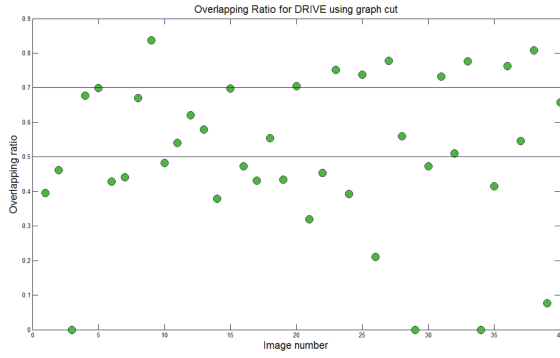


Fig. 9: Overlapping ratio distribution for the optic disc segmentation using traditional graph cut formulation.

Fig. 11: Overlapping ratio distribution for the optic disc segmentation using traditional graph cut formulation on MRF reconstructed images.

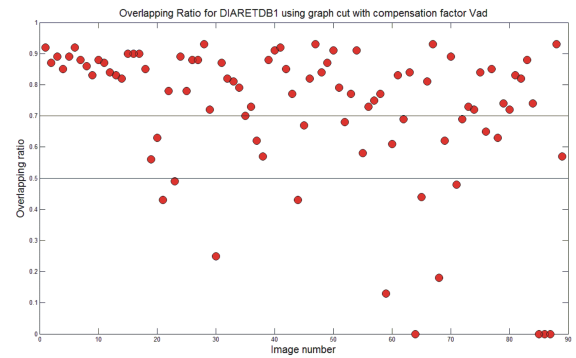
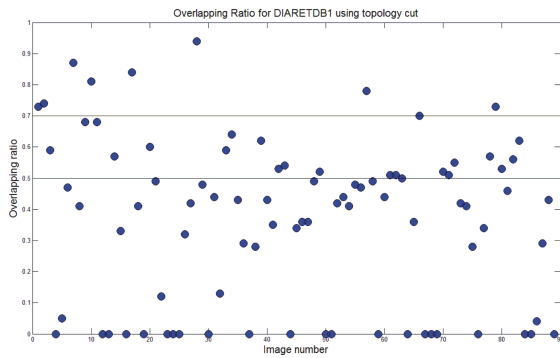
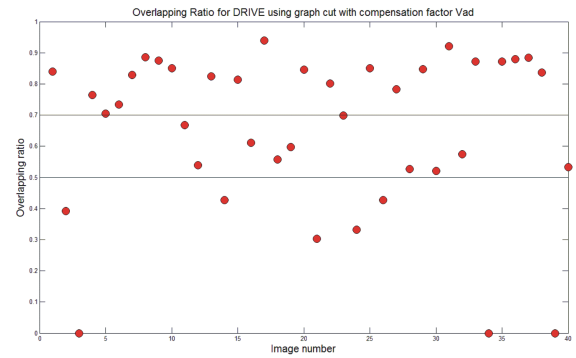
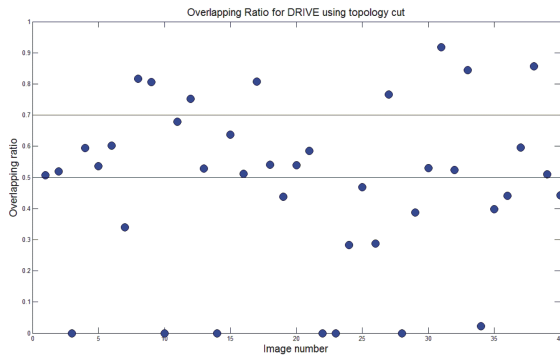


Fig. 10: Overlapping ratio distribution for the optic disc segmentation using topology cut technique.

Fig. 12: Overlapping ratio distribution for the optic disc segmentation using graph cut technique with compensation factor  $V_{ad}$ .

TABLE V: successful optic disc segmentation ( $Oratio > 50\%$ ) on DRIVE and DIARETDB1 using different methods.

| Method                                 | DRIVE         | DIARETDB1     |
|--|---------------|---------------|
| <b>Graph cut</b>                       | 21/40 = 52.5% | 47/89 = 52.8% |
| <b>Topology Cut</b>                    | 24/40 = 60.0% | 30/89 = 33.7% |
| <b>MRF + Graph Cut</b>                 | 36/40 = 90.0% | 62/89 = 69.6% |
| <b>Graph Cut with <math>Vad</math></b> | 32/40 = 80.5% | 77/89 = 86.5% |

the segmentation is compared with the hand labelled image. In the case of a perfect matching,  $Oratio = 1$ , for all the images in the dataset the area under the curve would be zero. Since our method shows the minimum area under the curve, it is clear that graph cut technique using the compensation factor  $Vad$  outperforms other techniques. The cumulative histograms provide a summary of the success of our method.

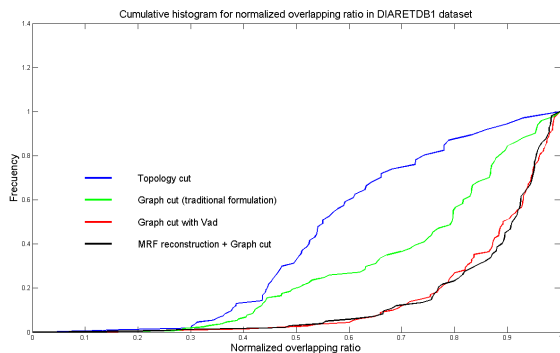


Fig. 13: Cumulative histogram for normalized overlapping ratio on DIARETDB1 dataset using different methods.

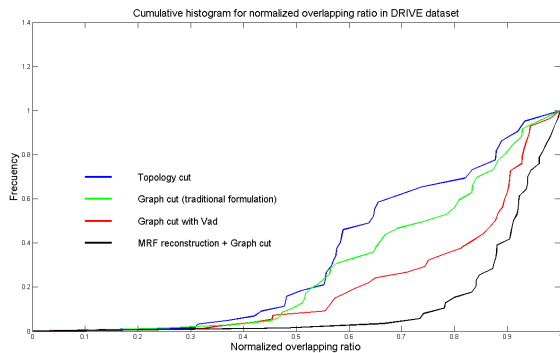


Fig. 14: Cumulative histogram for normalized overlapping ratio on DRIVE dataset using different methods.

### A. Discussion

Results are very clear, both methods have outperformed other methods in the literature. From tables III and IV it is possible to observe the performance of both methods on DIARETDB1 and DRIVE datasets.

In the case of DIARETDB1, “MRF + graph cut” method performs slightly better than “Graph Cut with  $Vad$ ” method by 2.56%. The outperformance is more visible in the case

of DRIVE dataset, where the “MRF + graph cut” method reached an average overlapping ratio of 11.5% more than “Graph Cut with  $Vad$ ” method.

Nevertheless “MRF + graph cut” method produced a considerable amount of null segmentation when performing on DIARETDB1. While “Graph Cut with  $Vad$ ” method produced only four cases of null segmentation.

The ideal conditions for the performance of “MRF + graph cut” method are that blood vessels have been detected with high confidence, then the reconstruction will produce a well defined optic disc and as a consequence a good segmentation will be achieved. On the other hand if the retinal image do not have the best conditions to perform the segmentation of vessels (e.g. severe damaged retina) the reconstruction will not offer a well defined object to segment and consequently the segmentation will not succeed.

In general the DIARETDB1 images are characterized by contain at least one sign of retinal lesion. This complicates the analysis of the images (blood vessels and optic disc segmentation), but precisely these type of images are the main concern in a retinal test.

The “Graph Cut with  $Vad$ ” method performs the segmentation using the original data in the image. This method permits that misclassified vessel pixels (false positives and false negatives) are part of the graph as well, and with the declaration of seeds the optimal segmentation is found.

In general the optic disc on DRIVE dataset is segmented better by “MRF + graph cut” method; while “Graph Cut with  $Vad$ ” method produced better segmentation of the optic disc on DIARETDB1 dataset.

## VIII. CONCLUSIONS

Optic disc segmentation is an important process in the analysis of retinal images. The analysis of optic disc morphology is part of the retinal screen process. Retinal Blood vessel network requires special attention due to its overlapping with the optic disc. In this paper we have presented two methods for the segmentation of the optic disc based in the graph cut technique. We followed the two major premises: incorporating vessels into the graph formulation and masking them out prior to its segmentation by applying a MRF reconstruction.

The methods were tested in two public data sets: DIARETDB1 and DRIVE. The results were compared with the results of the traditional formulation of the graph cut and the topology cut techniques.

## REFERENCES

- [1] R. Chrastek, M. Wolf, K. Donath, H. Niemann, D. Paulus, T. Hothorn, B. Lausen, R. Lammer, C. Y.

- Mardin, and G. Michelson. Automated segmentation of the optic nerve head for diagnosis of glaucoma. *Medical Image Analysis*, 9(1):297–314, 2005.
- [2] A.A. Efros and T.K. Leung. Texture synthesis by non-parametric sampling. *In Proceedings of the ICCV*, pages 1033–1038, 1999.
- [3] A. Aquino et al. Detecting the optic disc boundary in digital fundus images using morphological, edge detection and feature extraction techniques. *IEEE transactions on medical imaging*, 29(10):1860–1869, 2010.
- [4] T Kauppi, V Kalesnykiene, J Kamarainen, L Lensu, I Sorri, A Raninen, R Voitalainen, H Uusitalo, H Kalvainen, and J Pietila. Diaretdb1 diabetic retinopathy database and evaluation protocol. *In Proceedings of British Machine Vision Conference.*, 2007.
- [5] J. Lowell, A. Hunter, D. Steel, A. Basu, R. Ryder, E. Fletcher, and L. Kennedy. Optic nerve head segmentation. *IEEE Transactions on Medical Imaging*, 23(2):256–264, 2004.
- [6] M. Niemeijer, M. D. Abramoff, and B. van Ginneken. Segmentation of the optic disc, macula and vascular arch in fundus photographs. *IEEE Transactions on Medical Imaging*, 26(1):116–127, 2007.
- [7] A. Salazar-Gonzalez, Y. Li, and X. Liu. Retinal blood vessel segmentation via graph cut. *In Proceedings of the 11th International Conference on Control, Automation, Robotics and Vision, ICARCV*, 1:225–230, 2010.
- [8] A. Salazar-Gonzalez, Y. Li, and X. Liu. Optic disc segmentation by incorporating blood vessel compensation. *In Proceedings of IEEE SSCI, International Workshop on Computational Intelligence In Medical Imaging*, pages 1–8, 2011.
- [9] Clara I. Sanchez, Maria Garcia, Agustin Mayo, Maria I. Lopez, and Roberto Hornero. Retinal image analysis based on mixture models to detect hard exudates. *Medical Image Analysis*, 13:650–658, 2009.
- [10] J. Staal, M. D. Abramoff, M. Niemeijer, M. A. Viergever, and B. van Ginneken. Ridge-based vessel segmentation in color images of the retina. *IEEE Transactions on Medical Imaging*, 23(4):501–509, 2004.
- [11] D. Welfer, J. Scharcanski, C. Kitamura, M. Dal Pizzol, L. Ludwig, and D. Marinho. Segmentation of the optic disc in color eye fundus images using an adaptive morphological approach. *Computers in Biology and Medicine*, 40(1):124–137, 2010.
- [12] A. Youssif, A. Ghalwash, and A. Ghoneim. Optic disc detection from normalized digital fundus images by means of a vessels’s directed matched filter. *IEEE Transactions on Medical Imaging*, 27(1):11–18, 2008.
- [13] Y. Zeng, D. Samaras, W. Chen, and Q. Peng. Topology cuts: a novel min-cut/max-flow algorithm for topology preserving segmentation in n-d images. *Journal of computer vision and image understanding.*, 112(1):81–90, 2008.